Mathematical Biosciences and Engineering

MBE, 17 (3): 1944–1958.
DOI: 10.3934/mbe.2020103
Received: 31 July 2019
Accepted: 27 November 2019
Published: 19 December 2019

http://www.aimspress.com/journal/MBE

Research article

A novel compliant surgical robot: Preliminary design analysis

Akim Kapsalyamov [1], Shahid Hussain [2] and Prashant K. Jamwal [1]

[1] Department of Electrical and Computer Engineering, Nazarbayev University, Astana, Kazakhstan
[2] Human-Centred Technology Research Center, Faculty of Science and Technology, University of Canberra, Canberra, ACT, Australia

* **Correspondence:** Email: prashant.jamwal@nu.edu.kz; Tel: +7(7172)-705730.

Abstract: A robotic surgical system capable of performing minimally invasive surgery (MIS) is proposed in this paper. Based on the requirements of MIS, a compliant, seven- degrees of freedom (7-DOF) pneumatically actuated mechanism is designed. A remote center of motion (RCM) as a parallelogram mechanism for holding the laparoscopic camera is also developed. The operating workspace of robotic surgical system is determined considering the physical constraints imposed by mechanical joints. The simulation results show that the robotic system meets the design requirement. This research will lay a good foundation for the development of a compliant surgical robot to assist in MIS.

Keywords: medical robots; minimally invasive surgery; laparoscopic camera; remote center of motion; pneumatic actuator

1. Introduction

Minimally invasive surgery (MIS), which requires few small incisions (usually less than one inch in diameter), is preferred over open surgery owing to many advantages such as less tissue damage, reduced pain leading to quicker healing, and faster return to work. This procedure, therefore, has become a popular method during the last decades. Despite increased use, MIS has many challenges to meet and therefore it is also an important area of the surgical research. Few examples of MIS include heart surgery, breast surgery and endoscopic surgery [1].

The operating procedures are technically difficult and complex, because the human physiological anatomy is extremely complicated and there are many sensitive organs and tissues to be avoided. The puncture needle's initial position and the aspiration path are very precise in the

procedure of surgical treatment, which puts high demands on surgeons. This technical difficulty undoubtedly limits minimally invasive spinal treatment promotion and popularity [2]. The surgical robotics technology is the key to solve such issues in MIS. Robots can perform accurate positioning under manual or automatic operation. Moreover, they can be used for clamping/holding surgical instruments after their joints are locked, which provides a stationary and reliable platform for doctors to perform MIS.

In the past two decades, significant efforts have been done in order to design surgical robots [3–6]. Two of the major achievements in this field are "ZEUS" and "DA VINCI" surgical robots [7]. Tele-surgery is one of the most important applications of surgical robots, in which there are two subsystems, master and slave, which are connected with each other and with patient's body in desired spatial distances [8,9].

These surgical robots closely interact with human organs; therefore, safety is a key concern. Safe human tissue-robot interaction could be achieved by either designing appropriate robot control algorithms or by using compliant robotic mechanisms [10]. Recently, there has been an increasing trend of designing robots for MIS by using compliant actuation concepts [5,6,10]. In this paper a novel compliant mechanism of a robot for MIS is presented. The surgical robot utilizes compliant pneumatic actuators in order to provide safe human tissue-robot interaction. Kinematic analysis is also carried out in order to establish the feasible workspace of the proposed surgical robotic mechanism. This work is a step forward towards the design of compliant robotic mechanisms for MIS surgery.

2. Surgical robot design

2.1. Robotic system for laparoscopic surgery

Key objectives such as reduced/compact size, compliant and lightweight manipulation, precision and accuracy are important while designing surgical robots [11–13]. Intuitively, compliant actuation and small sized robots with reduced power requirement can offer safe human tissue-robot interaction and ergonomic advantages compared to large, stiff and powerful robots for surgical applications [14]. Active surgical work volumes are often quite small, and scaling the mechanism accordingly is necessary. Therefore, a surgical robot for MIS with reduced scale is developed during this research.

The surgical tools and a laparoscopic camera are handled by the robotic manipulator. According to the surgical tool positioning and orientation that the surgical intervention is required to achieve, a mechanical structure of the robot is also designed. Robot arm performs the position control whereas the orientation control of the surgical tool is carried out by the robot wrist. The wrist also adjusts the orientation with respect to the arm since the arm position change affects tool orientation. Effective mechanical design not only accomplishes the surgical tasks, but also reduces the dependence relations between robot arm and its wrist, while enhancing the tracking velocity, for the safety of the operation [15].

2.2. Design of root arm

Surgical robot arm design should meet the requirements laid by surgeons, operating tasks, and the operating environments. A suitable relationship of the robot arm and of the wrist is also needed.

On the whole, the robot arm should be designed to meet the following requirements:

- Must have compliant actuation/manipulation
- Large workspace of the robot with reduced size of the robot structure
- The robot arm could achieve highly precise positioning
- Arm structure meets environmental requirements of the operation
- The safety must be guaranteed

It is required that a surgical robot arm is capable of reaching any position within the operating space [16]; therefore, robot arm must have at least three degrees of freedom (DOF). Currently, the robot arm patterns typical structure includes: articulated configuration, cylindrical configuration, SCARA configuration, Cartesian configuration, and polar configuration. These structure patterns can be compared according to joints and the movement axes of different combinations. The structural requirements for surgical robot includes; the large workspace, safe interaction with human tissues and organs, a small-sized structure, high-precision positioning, user friendly, and small influence of the arm movement to tool orientation. MIS robotic arm structures mostly utilize cylindrical configuration, SCARA configuration and Cartesian configuration [17]. For example:

- The US Integrated Surgical System Company developed ROBODOC system which utilized cylindrical configuration
- American Compute Motion Company "ZEUS" robot surgical system utilized SCARA configuration
- Switzerland Swiss Federal Research Institute for neurosurgery three-dimensional orientation surgical robot used Cartesian configuration [18]

Cylindrical configuration is smaller and has larger workspace, higher precision positioning and is user friendly. In Cartesian configuration, the two joints are level, which results in ease of movement. The orthogonal joints are cumbersome, which cause greater friction force than rotary joints [19]. The last joint of SCARA configuration rotary joints will cause relatively large inertial force, affecting the precision of surgical tool. Cylindrical configuration itself is smaller and provides larger work space, with higher precision positioning.

The robot must have sufficient strength, accuracy, safety [20] and dexterity for its intended use. For these purposes and other purposes different types of bearings were used in all of the rotational joints.

Based on the above analysis of operating space and requirements of operation, an articulated manipulator robot is designed as shown in Figure 1. As it can be seen from Figure 1, the robot arm consists of 2DOF shoulder, upper arm, forearm and a single DOF elbow between them. The shoulder implements abduction/adduction and flexion/extension movements and an elbow also give flexion/extension motion possibility for the surgical robotic manipulator.

2.3. Robot wrist design

The orientation of the surgical tools is achieved by controlling the robot wrist. Wrist joints on the basis of its structure can be divided into rolling joints and bent joints whereas on the basis of different assemblage ways of rotation joints, the wrist structures can be divided into one, two and three DOF [21]. The basic two DOF wrist and three DOF wrist structures are shown in Figure 2.

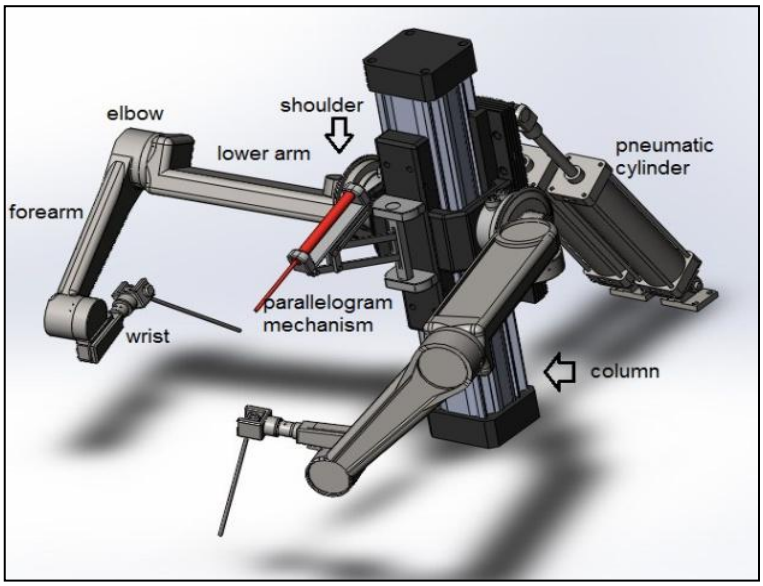

Figure 1. Assembly of the proposed surgical robot.

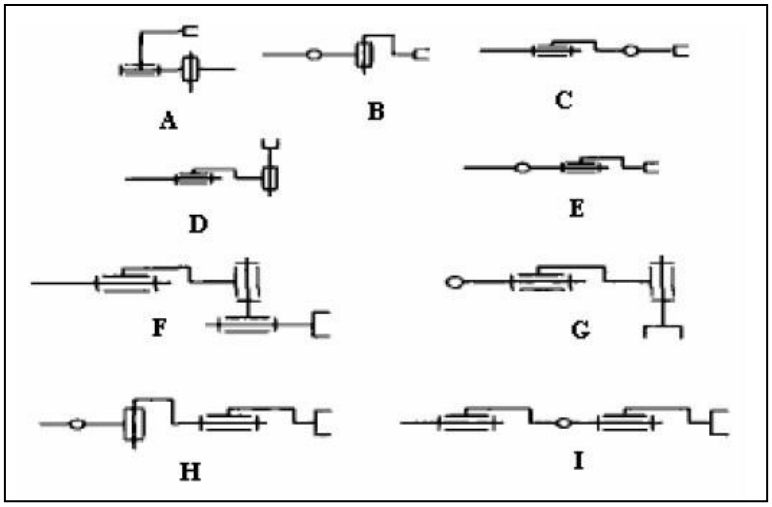

Figure 2. Two DOF wrist (A-E) and three DOF wrist (F-I).

The two DOF wrist mechanical structures are simple as compared to three DOF but three DOF has upper hand in attaining any posture but lacks behind the two DOF in simple control system. The angle of the tool can be changed in a definite range; therefore, it will meet the requirements of the surgical tool posture i.e. as soon as the surgical tool can rotate around the spherical surface when the entry point of the tool is determined.

Therefore, the robot wrist is designed with three DOF and the schematic is shown below on the Figure 3 (DOF indicated as $\theta_{5,}\theta_6$ and θ_7). Articulated seven DOF robot was designed as shown in Figure 1. The schematic of all the seven DOF are shown on the Figure 3. Four DOF are robot arm control and three DOF for the wrist orientation. The first DOF of the arm is for the vertical movement, the remaining three DOF of the arm are responsible for shoulder movements and rotation in the level plane. The three DOF decide the position of the tool in the selected working plane. The

last three DOF are for controlling the robot's wrist, which can control the required position of surgical tools within workspace.

All the six DOF of arm are powered with the help of rotary pneumatic actuators of different sizes and capacities. This designed mechanical structure has small-size, large workspace, high-precision positioning and ease in operations. A simple arm and wrist coupling relationship makes the kinematics analysis of the robot simple.

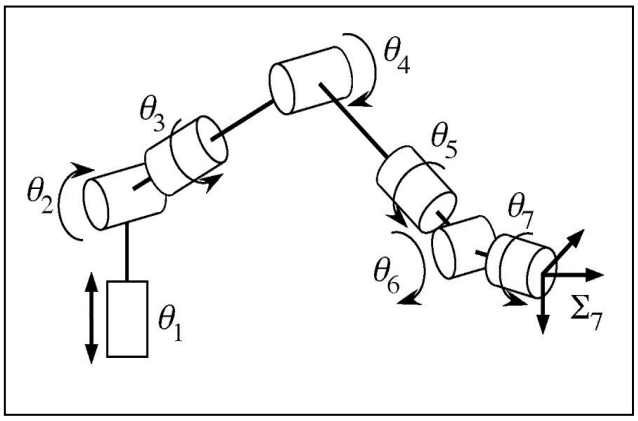

Figure 3. Schematic of Robot DOF.

The length of the lower arm is 330 mm, forearm is around 280 mm and the length of the wrist is 110 mm. The maximum length of each arm (including wrist) is kept as 720 mm.

2.4. Column

The column (Figure 1) allows vertical movements for the whole assembly, thus giving it the first DOF. Since the weight of the surgical robotic system is placed on the column, it requires a high power for vertical movements. For this purpose, two linear cylindrical pneumatic actuators which are capable of lifting large weights were used. Column has a height of 63 cm and allows all three arms to move about 30cm up and down.

2.5. RCM and parallelogram mechanism for laparoscopic camera

Because laparoscopy is performed through small incisions in the patient's body, robotic systems for MIS must pivot the surgical tools about these incisions [22] (Figure 4). This pivoting constraint is called a Remote Center-of-Motion (RCM), and it is an important task for any surgical system [23,24]. There are two ways to achieve RCM, one is implied by kinematic redundancy control, but the reliability and stability requirement for hardware and algorithms is high [25,26]. The safety of this method is low and few medical robots are controlled by this way, such as DLR MIRO surgical robot [27–29], Telelap XALF[30] Surgical robot. Another way is the mechanism constraint, such as passive joint, parallelogram mechanism, spherical mechanism, circular mechanism [31].

A manipulator with the proposed parallelogram mechanism (Figure 1) is shown for high speed and high precision pick-place task. In order to make the workspace larger, a rotational joint is added between the base and the proposed mechanisms. The mechanism gives 2 DOF to the system.

The laparoscopic camera is inserted into the patient's body via a trocar, and it transmits images of a wide operative field using an RF signal [32].

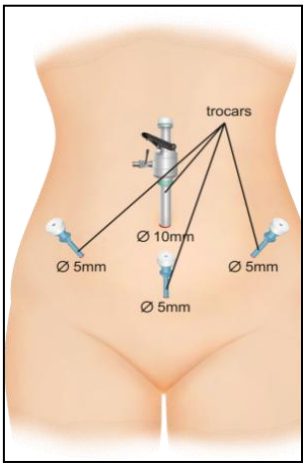

Figure 4. Incisions made by laparoscopes.

3. Kinematics of the robotic arm

3.1. Trocar point kinematics

The trocar point of the robot arm in the surgical robot functions as an end effector. The root-mean-square error (RMSE) must be calculated for the trocar point end position to ensure that robot arm acts in acceptable range [33]. This range accuracy is around several millimeters for the surgeon after 1-hour surgery work [34]. This project is aimed to outperform the success of human interaction in the surgery process. For the pneumatic actuators used in this arm, the position inaccuracy is 7.87–9.95 nanometers. However, it is directly proportional to the position and moment applied at a specific joint. The uncertainty of the final position increases as every joint is forced upon maximum torque [35].

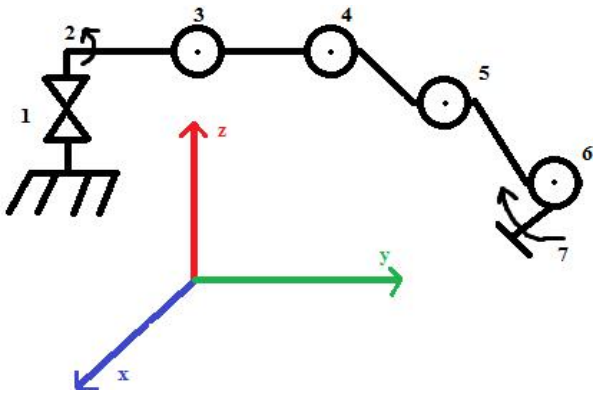

Figure 5. 7- DOF robotic surgery arm.

Figure 5 shows seven joints of robotic arm, while only one joint is translational. The following nomenclature was used to derive mathematical equation to find RMSE value of the robotic arm. Each joint was used to form the control of arm positioning independently in Cartesian form and assumed to be rigid in connection:

1. $\{x_c, y_c, z_c, \theta_c\}$ - *column translation motion;*
2. $\{x_{s1}, y_{s1}, z_{s1}, \theta_{s1}\}$ - *shoulder 1 rotational motion in* xy *plane;*
3. $\{x_{s2}, y_{s2}, z_{s2}, \theta_{s2}\}$ - *shoulder 2 rotational motion in* yz *plane;*
4. $\{x_e, y_e, z_e, \theta_e\}$ - *elbow rotational motion in* xz *plane;*
5. $\{x_{w1}, y_{w1}, z_{w1}, \theta_{w1}\}$ - *wrist 1 rotational motion in* xy *plane;*
6. $\{x_{w2}, y_{w2}, z_{w2}, \theta_{w2}\}$ - *wrist 2 rotational motion in* yz *plane;*
7. $\{x_{w3}, y_{w3}, z_{w3}, \theta_{w3}\}$ - wrist 3 rotational motion in xz plane;

These variables create linear relation with final position of end effector, and then the described workspace can be written in matrix form:

$$W_{space} = \begin{bmatrix} x_c & y_c & z_c & \theta_c \\ . & . & . & . \\ . & . & . & . \\ x_{w3} & y_{w3} & z_{w3} & \theta_{w3} \end{bmatrix}$$

In addition, the rate change of each variable classified as:

$$R = \overline{W}_{space} = \begin{bmatrix} \overline{x}_c & \overline{y}_c & \overline{z}_c & \overline{\theta}_c \\ . & . & . & . \\ . & . & . & . \\ \overline{x}_{w3} & \overline{y}_{w3} & \overline{z}_{w3} & \overline{\theta}_{w3} \end{bmatrix}$$

With known factors, it is possible to reduce the variable calculation. The column is the vector variable which describes the motion of the robotic arm in z direction:

$$x_c = y_c = z_c = const \Rightarrow \overline{x}_c = \overline{y}_c = \overline{z}_c = 0$$

This approach bases on the plane location of the variables, so in similar way, other planar variables have at least one constant number, which have no effect to the moment change:

- Shoulder parts:

$$1) x_{s1} = y_{s1} = z_{s1} = const \Rightarrow \bar{x}_{s1} = \bar{y}_{s1} = \bar{z}_{s1} = 0$$
$$\therefore a_{s1} = \bar{\theta}_{s1}$$
$$2) \mathrm{y}_{s2} = const \Rightarrow \bar{y}_{s2} = 0$$
$$\therefore a_{s1} = \sqrt{\bar{x}_{s1}^2 + \bar{z}_{s1}^2 + \bar{\theta}_{s1}^2}$$

- Elbow joint:

$$z_e = const \Rightarrow \bar{z}_e = 0$$
$$\therefore a_e = \sqrt{\bar{x}_e^2 + \bar{z}_e^2 + \bar{\theta}_e^2}$$

- Wrist parts:

$$x_{w2} = y_{w3} = z_{w1} = const \Rightarrow \bar{x}_{w2} = \bar{y}_{w3} = \bar{z}_{w1} = 0$$

$$\therefore a_{wi} = \sqrt{\bar{g}_{wi}^2 + \bar{\theta}_{wi}^2} \quad \text{, where } i = 1,2,3 \text{ and } g = x, \mathrm{y}, \mathrm{z} \text{ for corresponding plane}$$

Hence, the offset for the robot hand in z direction is:

$$d_{offset} = z_c$$

The mathematical approach for system linear equations based on Euclidean disjoint matrix transformation [36]:

$$D_{final} = W_{space} * k_{shift} \tag{1}$$

The shifted coefficient (k_{shift}) is the linear model of systematic variables, which depends on the positions and moment change of every joint. It shows the sum of the local positioning and orientation:

$$k_{shift} = \oint \oint \oint k_i d(x,y,z) + \int_0^{2\pi} \theta * (2\tau - \theta)\, d\,\theta, \text{ where } \tau = \tan^{-1}\frac{\mathrm{b_i}}{\mathrm{l_i}} \text{ (angular positional change)}$$

The angular positional change shows the orientation for the next joint in radians [37] and is calculated using cosine rule (Figure 6) [38]:

$$b_i = \sqrt{a_i^2 + c_i^2 - 2ac\cos(\alpha)} \text{ and for small change in radians}$$
$$\gamma << \alpha, \mathrm{l}_i = \sin(\frac{b}{c}\mathrm{d}_{offset} + \mathrm{atan}^{-1}(\beta + \alpha - \pi))$$

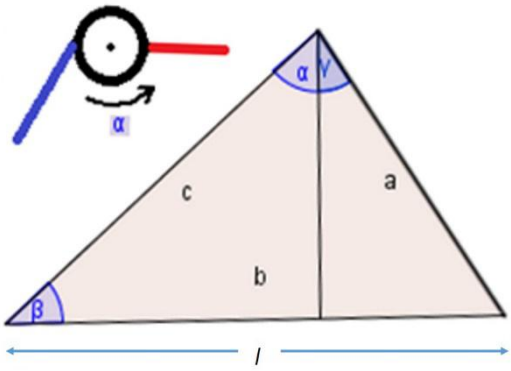

Figure 6. Cosine rule for rotational joint.

Analogously, all the joint shifts calculated in this manner and then final coefficient is obtained:

$$k_{shift} = \begin{bmatrix} x_c & y_c & z_c & \theta_c \\ x_{s1} & y_{s1} & z_{s1} & \theta_{s1} \\ x_{s2} & y_{s2} & z_{s2} & \theta_{s2} \\ x_e & y_e & z_e & \theta_e \\ x_{w1} & y_{w1} & z_{w1} & \theta_{w1} \\ x_{w2} & y_{w2} & z_{w2} & \theta_{w2} \\ x_{w3} & y_{w3} & z_{w3} & \theta_{w3} \end{bmatrix}'' * R + W_{space} * \begin{bmatrix} a_c \\ a_{s1} \\ a_{s2} \\ a_e \\ a_{w1} \\ a_{w2} \\ a_{w3} \end{bmatrix}$$

The Eq. (1) gives final position result for ideal case which is practically impossible. However, the above derivation suggests that the practical value of the final position depends on the second derivative of the workspace variables. Discrete joint variables undergo an uncertainty in Favorov method [39]:

$$k'_{shift} = k_{shift}\tilde{d}_{c,i}$$

Here $\tilde{d}$ is maximum uncertainty of the each joint. Finally, the RMSE value is obtained by following formula [40]:

$$RMSE = \sqrt{\frac{\sum W^2_{space}(\mathrm{x}_i, \mathrm{y}_i, \mathrm{z}_i, \theta_i) - k'_{shift} R(\mathrm{x}_i, \mathrm{y}_i, \mathrm{z}_i, \theta_i)}{7}} \tag{2}$$

3.2. Laparoscopic camera holder

Camera holder is connected through the parallelogram mechanism to the column, which reduces effect of the gravity to the holder. For small objects as laparoscopic camera attached, that effect is very small [41]. Then, uncertainty for this holder is due to the column and holder actuator (Figure 7):

$$RMSE = \sqrt{\frac{\sum W^2_{space}(\mathrm{x}_i, \mathrm{y}_i, \mathrm{z}_i, \theta_i) - k'_{shift} R(\mathrm{x}_i, \mathrm{y}_i, \mathrm{z}_i, \theta_i)}{3}} \tag{3}$$

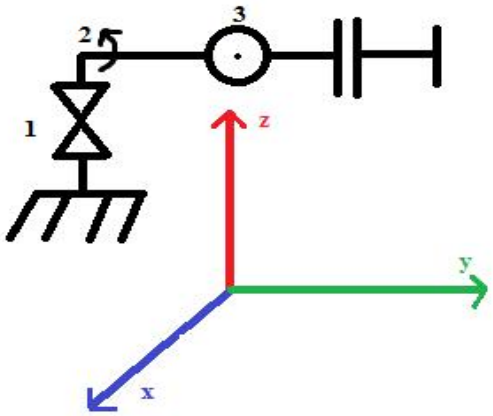

Figure 7. Free body diagram of holder joints.

3.3. Robot arm simulation

For the efficient use of this surgical robot, the column must be adjustable along the operating table. For a specific alignment, Eq. (1) gives the workspace as in Figure 8. The intersection of this workspace with human body consists $A_w = 93.45cm^2$ and for camera it is $A_c = 202.34cm^2$. Due to the fact that $A_c > 2A_w$, the laparoscopic camera can reach to any point of the human body, where the robotic arm operates (Figure 9).

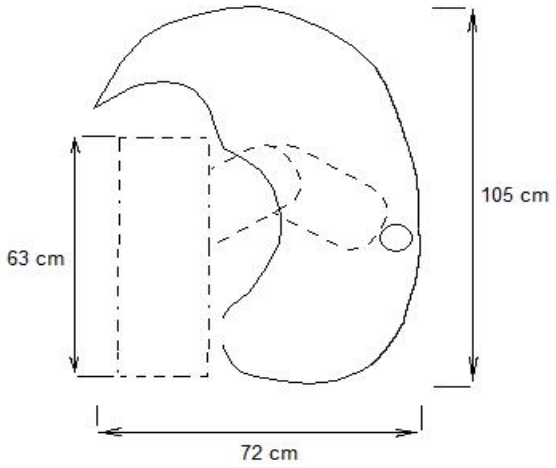

Figure 8. Workspace for robotic arm and laparoscopic camera holder.

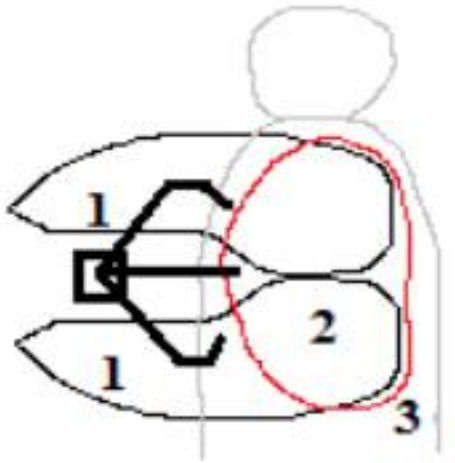

Figure 9. 1) Robotic arm workspace, 2) camera holder workspace, 3) body.

Mas-Coma et.al showed that the efficiency of the human concentration for any specific task decreases by exponential form because of neurological neurons [42]:

$$efficiency = ke^{0.03(t^2-2t)\alpha^{-8\beta}}$$

This equation indicates that human efficiency slows down faster in 2-hour work. The surgical robotic arm, in turn, works in constant efficient way with an uncertainty as in Eq. (2). This is illustrated in Figure 10.

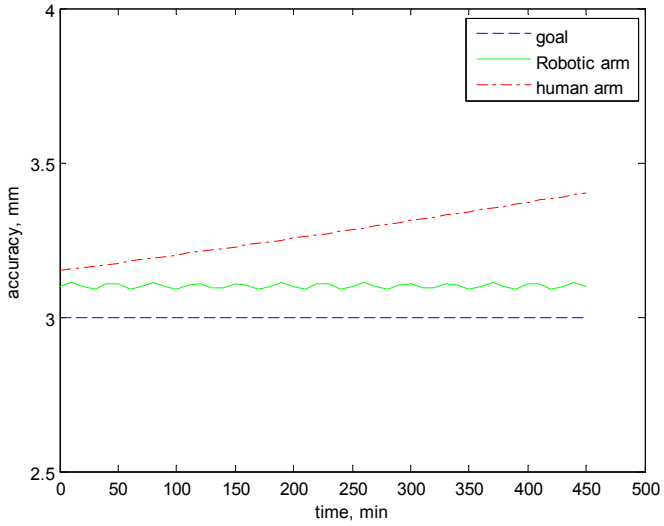

Figure 10. 1) Robotic arm workspace, 2) camera holder workspace, 3) body.

The Eq. (2) also indicates that the robotic arm RMSE reaches maximum point when the column has large offset value. This is explained in terms of enlarging workspace for robotic arm (Figure 11).

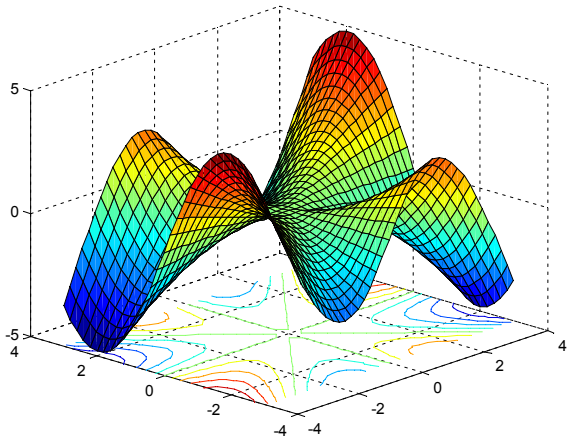

Figure 11. RMSE values for robotic arm workspace.

4. Conclusion

A novel compliant robotic mechanism is designed to enable manipulation of different kinds of surgical tools about a pivot point. These tools are commonly used in MIS such as therapy laser delivery tools, biopsy, colon cancer resection and brachytherapy needles [1,43]. The robot's special configuration enables it to reorient a surgical tool about a pivot point; achieve and control small-scale movement for precision manipulation in two independent degrees of freedom, and allow for miniaturization so it can overcome problems associated with the limited surgical workspaces. The manipulator can be used in manual, autonomous or remote-control modes. The special features of the proposed mechanism make it well suited for use in a broad range of medical interventions.

The designed surgical robotic mechanism has the following physical properties:

1. Mass: 17.6 kilograms
2. Length: (stretched arm): 330mm + 280mm + 110mm = 720mm

Overall, the desired design requirements were successfully achieved during this research and robot prototype development.

In conclusion, a 7-DOF robotic system for laparoscopic instruments and camera manipulation during MIS surgery is presented in this paper. Orientation of the trocar points mounted to the robotic system can be controlled in pitch, yaw and roll angles. Insertion depth of the laparoscope can also be controlled. All joint motions were decoupled to reduce control complexity as well as potential errors. Pitch and yaw motions of the laparoscope are controlled by a parallelogram mechanism driven by tendon in which a remote center of motion (RCM) can be created to passively protect the patient from injuries. The workspace of the robotic system bounded interaction forces between the robotic manipulator and the patient to certain thresholds, passively and actively. In future, further improvements in the designed mechanism shall be carried out besides design of control methods and interfaces as well as clinical trials.

Acknowledgments

This work was supported by the Faculty Development Competitive Research Grants,

Nazarbayev University, under Grant 090118FD5322.

Conflict of interest

The authors declare no conflict of interest.

References

1. W. Peh, CT-guided percutaneous biopsy of spinal lesions, *Biomed. Imag. Interv. J.*, **2** (2006), e25.
2. S. Yinhao, A. Gang, Z. Jianxun, C. Yanqiu, Medical robotic system for minimally invasive spine surgery, *2nd International Conference on Bioinformatics and Biomedical Engineering*, **2008** (2008), 1703–1706.
3. D. E. Ott, Unique laparoscopic access port for improving gas delivery, quality and surgical outcomes, *J. Med. Devices,* **8** (2014), 030916.
4. A. Talasaz, A. L. Trejos, S. Perreault, H. Bassan, R. Patel, A dual-arm 7-degrees-of-freedom haptics-enabled teleoperation test bed for minimally invasive surgery, *J. Med. Devices*, **8** (2014), 041004.
5. A. Pourghodrat, C. Nelson, D. Oleynikov, Electrohydraulic robotic manipulator with multiple instruments for minimally invasive surgery, *J. Med. Devices*, **8** (2014), 030919.
6. A. Pourghodrat, C. Nelson, Miniature fluidic actuators for surgical robotics, *J. Med. Devices*, **8** (2014), 030920.
7. H. Kumon, M. Murai, S. Baba, Endourooncology: New horizons in endourology, *Springer*, (2010), 39–46.
8. M. Hadavan, A. Mirbagheri, H. Salarieh, F. Farahmand, Design of a force-reflective master robot for haptic telesurgery applications: Robomaster1, *Conf. Proc. IEEE Eng. Med. Biol. Soc.*, **2011** (2011), 7037–7040.
9. K. Y. Kim, H. S. Song, J. W. Suh, J. J. Lee, A novel surgical manipulator with workspace-conversion ability for telesurgety, *IEEE/ASME Transact. Mechatron.*, **18** (2013), 200–211.
10. R. E. Goldman, A. Bajo, N. Simaan, Compliant motion control for continuum robots with intrinsic actuation sensing, *IEEE International Conference on Robotics and Automation*, **2011** (2011), 1126–1132.
11. K. Cleary, C. Nguyen, State of the art in surgical robotics: Clinical applications and technology challenges, *Comput. Aided Surg.*, **6** (2001), 312–328.
12. A. E. Quaid, R. A. Abovitz, Haptic information displays for computer-assisted surgery, *Proc. IEEE Int. Conf. Robotics and Automation*, **2** (2002), 2092–2097.
13. D. Stoianovici, Robotic surgery, *World J. Urology*, **18** (2000), 289–295.
14. M. Jakopec, S. J. Harris, F. R. Y. Baena, P. Gomes, J. Cobb, B. L. Davies, The first clinical application of a hands-on robotic knee surgery system, *Comput. Aided Surg.*, **6** (2001), 329–339.
15. S. M. Sajadi, S. H. Mahdioun, A. A. Ghavifekr, Design of mechanical structure and tracking control system for 5 DOF surgical robot, *21st Iranian Conference on Electrical Engineering (ICEE),* **2013** (2013), 1–6.

16. B. F. Yousef, F. M. T. Aiash, A mechanism for surgical tool manipulation, *9th Asian Control Conference (ASCC)*, **2013** (2013), 1–5.
17. Y. Ping-Lang, K. Zhi-Wei, L. Tien-Sen, L. Chung-Wei, Development of a new safety-enhanced surgical robot using the hexaglide structure, *2004 IEEE International Conference on Systems, Man and Cybernetics (IEEE Cat. No.04CH37583)*, **3** (2004), 2162–2167.
18. J. Funda, R. Taylor, B. Eldridge, S. Gomory, K. Gruben, Constrained Cartesian motion control for teleoperated surgical robots, *IEEE Transact. Robot. Automat.*, **12** (1996), 453–465.
19. H. Seno, K. Kawamura, Y. Kobayashi, M. G. Fujie, Pilot study of design method for surgical robot using workspace reproduction system, *Conf. Proc. IEEE Eng. Med. Biol. Soc.*, **2011** (2011), 4542–4545.
20. B. Fei, W. S. Ng, The safety issues of medical robotics, *Reliab. Eng. Syst. Safety*, **73** (2001), 183–192.
21. Q. Du, Q. Huang, L. Tian, C. Liu, Mechanical design and control system of a minimally invasive surgical robot system, *International Conference on Mechatronics and Automation,* **2006** (2006), 1120–1125.
22. Y. Fu, G. Niu, B. Pan, K. Li, S. Wang, Design and optimization of remote center motion mechanism of minimally invasive surgical robotics, *IEEE International Conference on Robotics and Biomimetics (ROBIO),* **2013** (2013), 774–779.
23. R. C. O. Locke, R. V. Patel, Optimal remote center-of-motion location for robotics-assisted minimally-invasive surgery, *IEEE International Conference on Robotics and Automation*, **2007** (2007), 1900–1905.
24. L. Yang, C. B. Chng, C. K. Chui, D. Lau, Model-based design analysis for programmable remote center of motion in minimally invasive surgery, *IEEE Conference on Robotics, Automation and Mechatronics*, **2010** (2010), 84–89.
25. M. M. Dalvand, B. Shirinzadeh, Remote centre-of-motion control algorithms of 6-RRCRR parallel robot assisted surgery system (PRAMiSS), *IEEE International Conference on Robotics and Automation*, **2012** (2012), 3401–3406.
26. J. T. Wilson, T. Tsu-Chin, J. Hubschman, S. Schwartz, Evaluating remote centers of motion for minimally invasive surgical robots by computer vision, *IEEE/ASME International Conference on Advanced Intelligent Mechatronics*, **2010** (2010), 1413–1418.
27. U. Hagn, R. Konietschke, A. Tobergte, MiroSurge: A versatile system for research in endoscopic telesurgery, *Int. J. Comput. Assist. Radiol. Surg.*, **5** (2010), 183–193.
28. U. Hagn, M. Nickl, S. Jörg, The DLR MIRO: A versatile lightweight robot for surgical applications, *Industr. Robot Int. J.*, **35** (2008), 324–336.
29. R. Konietschke, U. Hagn, M. Nickl, S. Jörg, A. Tobergte, G. Passig, et al., The dlr mirosurge—a robotic system for surgery, *IEEE International Conference on Robotics and Automation*, **2009** (2009), 1589–1590.
30. M. Stark, T. Benhidjeb, S. Gidaro, The future of telesurgery: A universal system with haptic sensation, *J. Turkish-German Gynecol. Assoc.*, **13** (2012), 74–76.
31. H. Choi, H. J. Kim, Y. Lim, H. Kwak, J. Jang, J. Won, Conically shaped remote center-of-motion mechanism for single-incision surgery, *IEEE/RSJ International Conference on Intelligent Robots and Systems*, **2013** (2013), 3604–3609.

32. P. Li, H. M. Yip, D. Navarro-Alarcon, Y. Liu, C. F. M. Tong, I. Leung, Development of a robotic endoscope holder for nasal surgery, *IEEE International Conference on Information and Automation (ICIA)*, **2013** (2013), 1194–1199.
33. I. G. French, C. S. Cox, Modelling, design and control of a modern electropneumatic actuator, *IEE Proceedings D - Control Theory and Applications*, **137** (1990), 145–155.
34. K. Ikuta, T. Kato, H. Ooe, S. Ando, Surgery recorder system" for recording position and force of forceps during laparoscopic surgery, *IEEE/ASME International Conference on Advanced Intelligent Mechatronics*, **2007** (2007), 1–6.
35. J. Y. Lai, C. H. Menq, R. Singh, Accurate Position Control of a Pneumatic Actuator, *American Control Conference*, **1989** (1989), 1497–1502.
36. N. Kemmer, *Vector Analysis*, Cambridge University Press, 1977.
37. I. Uzmay, S. Yildirim, Geometric and algebraic approach to the inverse kinematics of four-link manipulators, *Robotica*, **12** (1994), 59–64.
38. S. Kadry, Mathematical Formulas for Industrial and Mechanical Engineering, *Elsevier*, (2014), 31–51.
39. S. Favorov, Discrete unbounded sets in a finite dimensional space and beyond, *Electron. Notes Discrete Math.*, **43** (2013), 389–395.
40. A. Zollanvari, E. R. Dougherty, Moments and root-mean-square error of the Bayesian MMSE estimator of classification error in the Gaussian model, *Pattern Recogn.*, **47** (2014), 2178–2192.
41. S. K. Agrawal, S. K. Banala, A. Fattah, V. Sangwan, V. Krishnamoorthy, J. P. Scholz, et al., Assessment of motion of a swing leg and gait rehabilitation with a gravity balancing exoskeleton, *IEEE Trans. Neural Syst. Rehabil. Eng.*, **15** (2007), 410–420.
42. S. Mas-Coma, V. H. Agramunt, M. A. Valero, Neurological and ocular fascioliasis in humans, *Adv. Parasitol.*. **84** (2014), 27–149.
43. J. L. Sun, S. Y. Xing, Short-term outcome of laparoscopic surgery versus open surgery on colon carcinoma: A meta-analysis, *Math. Biosci. Eng.*, **16** (2019), 4645–4659.

AIMS Press